WAVE-CURRENT INTERACTION AT A RIGHT ANGLE OVER ROUGH BEDS: TURBULENCE ANALYSIS

Massimiliano Marino[1], Rosaria Ester Musumeci[1], Carla Faraci[2]

In the present work, an investigation on the hydrodynamics of wave-current orthogonal combined flow has been carried out. The work focuses on the effects of the oscillatory flow superposed on the current steady boundary layer, and on how the oscillatory flow affects the current velocity distribution. A laboratory experimental campaign of wave-current orthogonal interaction has been carried out in a shallow water basin at DHI Water and Environment (Hørsholm, Denmark), in order to investigate the orthogonal combined flow in the presence of different roughness beds. Mean flow has been investigated by computing time- and space-averaged velocity profiles. Friction velocity and equivalent roughness have been inferred from the velocity profiles by best fit technique, in order to quantify the shear stress experienced by the current mean flow. Tests in the presence of only current, only waves and combined flow have been performed. Instantaneous velocities have been Reynolds-averaged in order to obtain turbulent fluctuations time series and compute turbulence related quantities, such as Reynolds stresses. The mean current velocity profiles have been also compared with a selection of analytical models in order to assess their validity for the case of wave-current orthogonal flow for the considered wave and current condition ranges. The analysis of the mean flow revealed a complex interaction of the waves and currents combined flow. Depending on the relative strength of the current with respect to the waves, the superposition of the oscillatory flow may determine an increase or a decrease of the bottom friction experienced by the current. Such a behavior is also strictly related to the bed physical roughness. Analysis of the turbulence Reynolds stresses seems to confirm the results of the mean flow investigation.

Keywords: nonlinear waves; turbulent flows; coastal hydrodynamics

INTRODUCTION

Waves and currents are usually simultaneously present in coastal waters. Their combined flow plays a fundamental role in several coastal processes such as sediment transport, mixing processes, diffusion etc. The influence of the waves on a current is strongly related to the processes taking place within the bottom boundary layer. Specifically, two boundary layers develop under a combined flow of waves and currents: an oscillatory boundary layer associated with waves, and a steady boundary layer generated by the current. The two flows feature very different time and length scales, resulting in a thin wave boundary layer close to the bed, being embedded in a larger, steady current boundary layer. The presence of the wave boundary layer has been found to significantly affect the bottom flow, determining the current to experience an 'apparent' roughness increase (Grant and Madsen, 1979), which affects its velocity vertical distribution. The interaction between the two bottom flows is however rather complex and highly nonlinear, therefore any scientifically relevant investigation should consider the simultaneous presence of both. In the near-shore, wave-current hydrodynamics is furtherly complicated by the interaction with the sea bed, which can be fixed or movable and feature the presence of time-evolving bedforms (e.g. ripples). In the last decades several studies contributed to the current knowledge of the wave-current interaction hydrodynamics, which includes laboratory, field and numerical investigations.

One of the earliest experimental campaign on a wave-current flume is the one by Bakker and Van Doorn (1978), which carried out a series of experiment of following waves and current over rough beds in a wave flume. Accurate bed shear stress measurements have been obtained. The investigation was mostly focused on the comparison of the suspended sand concentration observations with the predictions of a mathematical model by Bakker (1975).

Kemp and Simons (1982, 1983) conducted two experimental studies in a 10.00 m long wave flume, with waves propagating in the same and opposite direction with respect to the current. The investigation revealed that when waves and currents propagate in the same direction, the superposition of waves determines an increase of current mean velocities in proximity of a smooth bed, whereas over rough beds a reduction is always observed. Instead, when waves propagate opposite to the current, a reduction of the current intensity near the bed has been observed. The different behavior between smooth and rough beds has been explained as a change in the eddy pattern in-between the rough elements.

Mathisen and Madsen (1996a,b) carried out experiments of combined flow on a fixed ripple bed, showing that the bottom roughness for current alone, waves alone and wave-current bottom boundary layer flow can be characterised by a single roughness scale.

[1]Department of Civil Engineering and Architecture, University of Catania, Italy
[2]Department of Engineering, University of Messina, Italy

Lodahl et al. (1998) carried out experiments in a smooth oscillating water tunnel showing different shear stress patterns. If the flow regime is current dominated, i.e. the current mean velocity is larger than the wave orbital velocity, a linear relation between the wave-current shear stress and the wave motion Reynolds numbers occurs, whereas if the flow is wave dominated two different scenarios may follow. If the wave motion regime in the boundary layer is laminar a shear stress decrease occur, while if wave motion regime is turbulent, a bottom shear stress increase happens in comparison with the only current case.

An experimental campaign on an oscillating tunnel where co-linear waves and currents are generated over smooth, sandpaper and round marbles bottom has been carried out by Yuan and Madsen (2014). Results show that in the presence of regular waves a two-logarithmic structure of the velocity profile is observed, as predicted by the original Grant and Madsen (1979) model, whereas in the presence of weak currents opposing to nonlinear waves the two-logarithmic profile is suppressed by the boundary layer streaming induced by the asymmetric turbulence determined by the nonlinear waves.

The first combined flow experiments at a right angle reported are the ones by Bijker (1967). These experiment have been conducted in a 27.00 m x 17.00 m wave tank, in which tests have been performed in presence of fixed and movable beds. Detailed velocity measurements have not been carried out, although bed shear stresses have been measured and bedload sediment transport has been quantified by means of sediment traps. Based on the the results of these experiments, Bijker (1967) proposed empirical formulations for both shear stresses and sediment transport.

Visser (1987) presented a set of data of wave-current orthogonal interaction experiments in a wave basin, with a focus on the increase of the mean bottom stress due to the presence of waves. Mean and orbital velocity measurements have been carried out by means of a laser Doppler anemometer. The results were compared with the prediction of models by Bijker (1967) and Fredsøe (1984), with both models resulting to underestimate bottom shear stresses in comparison with the experimental evidence.

Sleath (1991) carried out experiments in a steady flow flume with a oscillating bed moving perpendicularly to the current, and measured velocity profiles by means of a laser Doppler anomemeter. Mean velocity profiles show agreement with the predictions of the models of Grant and Madsen (1979) and Christoffersen and Jonsson (1985) in the current boundary layer, with larger deviations in the wave boundary layer.

Musumeci et al. (2006) performed experiments of wave-current interaction at a right angle in a 18.00 x 3.60 m wave tank, over small and large roughness beds. The analysis on velocity profiles suggested that when waves are superposed to the current, an increase of near-bottom velocities occurs over smooth bed, the opposite happens in presence of a rough bed. Moreover, larger current velocities have been observed in proximity of the bottom in the waves plus current case and smaller in the current only case, in presence of small and the large roughness, respectively. Effects of current on waves have been investigated aswell. The strong turbulence induced by the current on the waves determines an homogenization of the wave velocity profile and reduces, or sometimes suppress, the steady streaming in the boundary layer. Moreover, in the small roughness case, apparent roughness k_s may decrease when waves are superposed on the current, whereas over large roughness beds, increase of k_s up to an order of magnitude has been observed.

Fernando et al. (2011) carried out perpendicular wave-current laboratory experiments in a 24.00 x 10.00 x 0.90 m wave basin over a movable bed. The evidences show that the current is always significantly modified by the superposition of waves, which induces a reduction of the near-bed current velocities due to an increase of the bed shear stress and apparent roughness. Moreover, Fernando et al. (2011) compared the experimental velocity data with a selection of analytical models. For waves with wave height to water depth ratio up to 0.45, models based on the reference point (such as Grant and Madsen (1986)) agree well with experimental findings, whereas the other generally underestimate the bed shear and apparent roughness. For waves with wave height to water depth ratio larger than 0.45 current velocity deviates significantly in the near-surface from the logarithmic law, which cannot be predicted by any of the considered models.

Lim and Madsen (2016) carried out a series of experiments on combined near-orthogonal current and waves over smooth and uniform ceramic-marbles bed. Three different condition are examined and compared (only currents, only waves and waves plus currents) and three different wave-current angles tests are performed (60, 90, 120 degrees) into a 3D experimental basin. The wave motion superimposed to an orthogonal smooth turbulent current determines an increase of the bottom mean velocity and a decrease of the bottom roughness. Over rough beds, the wave-current combined flow induce a reduction of the bottom mean velocity, as Grant and Madsen (1986) model predicts. However, results show that the model tends to overpredict influence of the wave motion on the current, especially in wave dominated regime, when the

angle of attack is different from collinear or near-orthogonal. This effect is amplified by the presence of bedforms which induce the current to veer at the bottom along the ripples direction.

Few studies with wave-current angles different than 0, 90 and 180 degrees exist, the already mentioned Arnskov et al. (1993), which included angles of 72 and 108 degrees, and Havinga (1992) and Lim and Madsen (2016), which performed experiments with 60 and 120 degrees angles.Recent studies investigated the interaction between steady orthogonal currents in presence of shoaling waves (Marino et al., 2020b,a).

Notwithstanding the large amount of literature on wave-current interaction, attention has been focused almost exclusively on the mean flow. Little has been reported to understand the combined flow with respect of the boundary layer turbulence activity. Nevertheless, a quantitative analysis of the turbulent properties of the wave-current flow is necessary to understand the bottom friction generation in proximity of the bed.

In the light of the above, the present study is aimed to purse the following objectives: (i) Provide new experimental datasets for orthogonal wave-current interaction A laboratory experimental campaign has been conducted in order to investigate the hydrodynamics of the combined flow, in the presence of different rough beds. The objective is to obtain new high-quality velocity and wave surface elevation datasets in order to assist the validation of analytical and numerical models for the case of orthogonal combined flow. (ii) Contribute to the understanding of the wave-current orthogonal hydrodynamics. To this aim, a study on the time-averaged characteristics of the combined flow has been conducted. Moreover, the present work pursue an attempt to analyze turbulence related quantities in the combined flow. This is carried out by means of recovering turbulent fluctuations from velocity time series and through analysis of Reynolds stresses.

EXPERIMENTS

A laboratory campaign has been carried out at DHI Water and Environment (HÃ¸rsholm, Denmark) in a three dimensional Shallow Water Basin, in the framework of an Hydralab+ Transnational Access project WINGS (Waves plus currents INteracting at a right anGle over rough bedS), funded by the EU Commission through the Hydralab+ programme. A selection of pictures of the basin is shown in Figure 1.

The basin (schematized in Figure 2) is 35 m long and 25 m wide, with a maximum depth of 1.00 m. On the longer side, the basin is provided with a multi-paddle piston-type wavemaker. The wavemaker front is 18.00 m wide, and consists of 36 paddles, with each paddle being 1.20 m high and 0.50 m wide. The presence of several independent paddles allows the wavemaker to reproduce different types of wave conditions: regular and irregular waves, 2D and 3D waves, sinusoidal or cnoidal, faced forward or inclined by a defined angle ranging from 30° to 90°. The wavemaker is able to generate waves from 0.05 up to 0.45 m of wave height.

In order to reduce wave reflection, a 18.75 m barrier made up by 15 parabolic steel absorbers is positioned 12.00 m away from the wavemaker. For the same purpose, a C-shaped coarse-grained material beach (d_{50} in the order of $O(10^{-2} \div 10^{-1}$ m) is located at the onshore end of the wave tank.

The water, for both filling and recirculation purposes, is brought from a local lake to a subterranean tank, in which three submerged pumps brings water into the tank. A recirculation system allows the generation of a current, which is conveyed into (out of) the basin through a 12 m inlet (outlet). An electromagnetic flowmeter having a 10^{-4} m^3s^{-1} precision allows to monitor the recirculation discharge. The still water level in the tank is measured by means of a physical meter stick.

The bottom of the basin is horizontal. In order to reproduce two different bottom rough conditions, a series of wood panels with fixed grains glued on top, are positioned on the tank bottom. Specifically, a series of panels with sand (SB) and a series with gravel (GB), with a grain diameter of d_{50} = 0.0012 m and d_{50} = 0.025 m respectively were installed. The panels cover a rectangular area of 7.50 x 5.00 m, which is called within the text the controlled roughness area. The controlled roughness area, for both sand and gravel panels, is shown in Figure 1c and d.

Water surface elevation is measured by means of 24 resistive wave gauges (WG, Figure 3a). The wave gauges are connected to a series of analog data loggers, which allows the adjustment of gauges resolution and sensitivity. The wave gauges are distributed all over the area in front of the wavemaker in order to give detailed spatial information about the wave field. Four out of 24 gauges (WG11 to 14) are positioned in order to measure wave reflection by means of the Faraci 4-probes reflection method (Andersen and Faraci, 2003). The wave gauges are shown in Figure 3a, whereas their coordinates in the basin are listed in Table 1.

Flow velocities have been measured by means of 5 Acoustic Doppler Velocimeters (ADV), the model

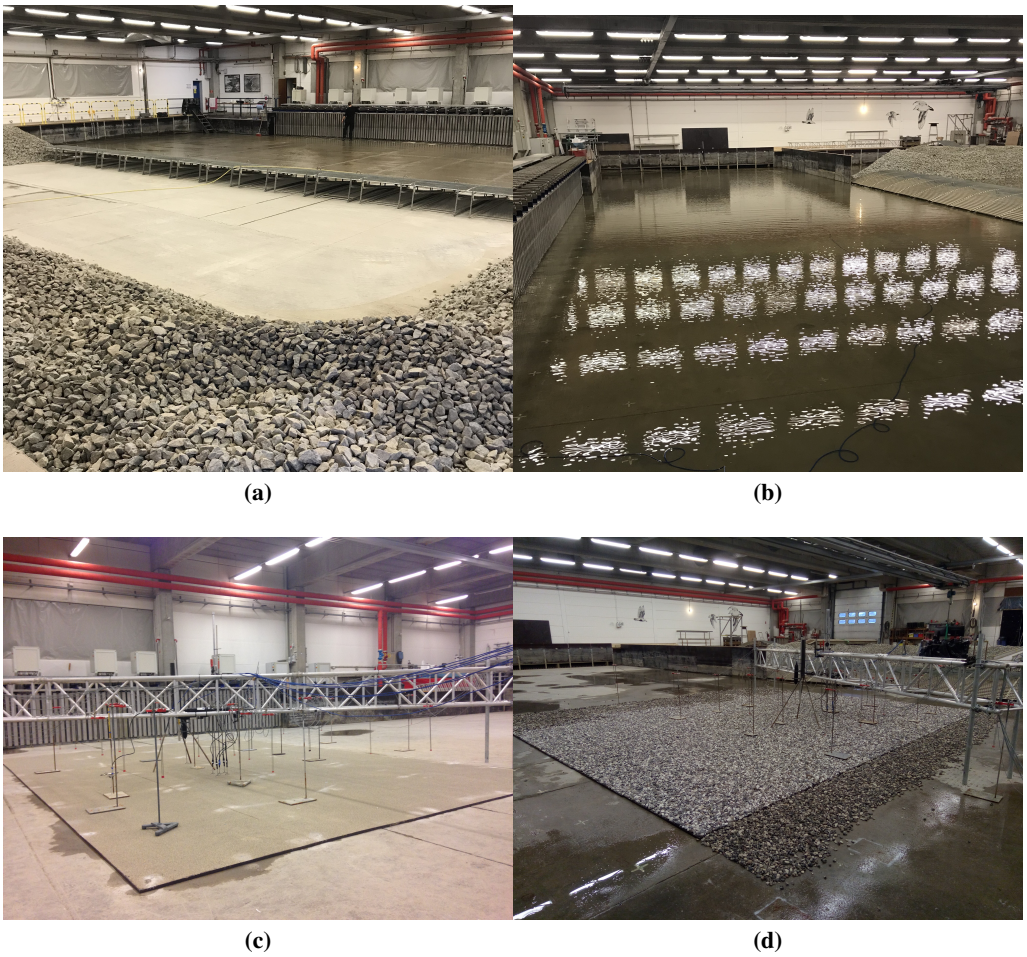

(a) **(b)**

(c) **(d)**

Figure 1: Pictures of the Shallow Water Basin: (a) empty basin from the coarse beach side, (b) full basin from the current outlet side, (c) sand bed panels, (d) gravel bed panels.

Table 1: Positions of the resistive wave gauges in the Shallow Water Basin.

Wave gauge	x [m]	y [m]	Wave gauge	x [m]	y [m]
WG1	13.50	4.00	WG13	18.00	7.02
WG2	13.50	6.00	WG14	18.00	7.46
WG3	13.50	8.00	WG15	18.00	8.00
WG4	16.00	4.00	WG16	19.00	6.20
WG5	16.00	5.00	WG17	19.50	4.00
WG6	16.00	6.00	WG18	19.50	5.00
WG7	16.00	7.00	WG19	19.50	6.00
WG8	16.00	8.00	WG20	19.50	7.00
WG9	18.00	4.00	WG21	19.50	8.00
WG10	18.00	5.02	WG22	21.50	4.00
WG11	18.00	6.60	WG23	21.50	6.00
WG12	18.00	6.78	WG24	21.50	8.00

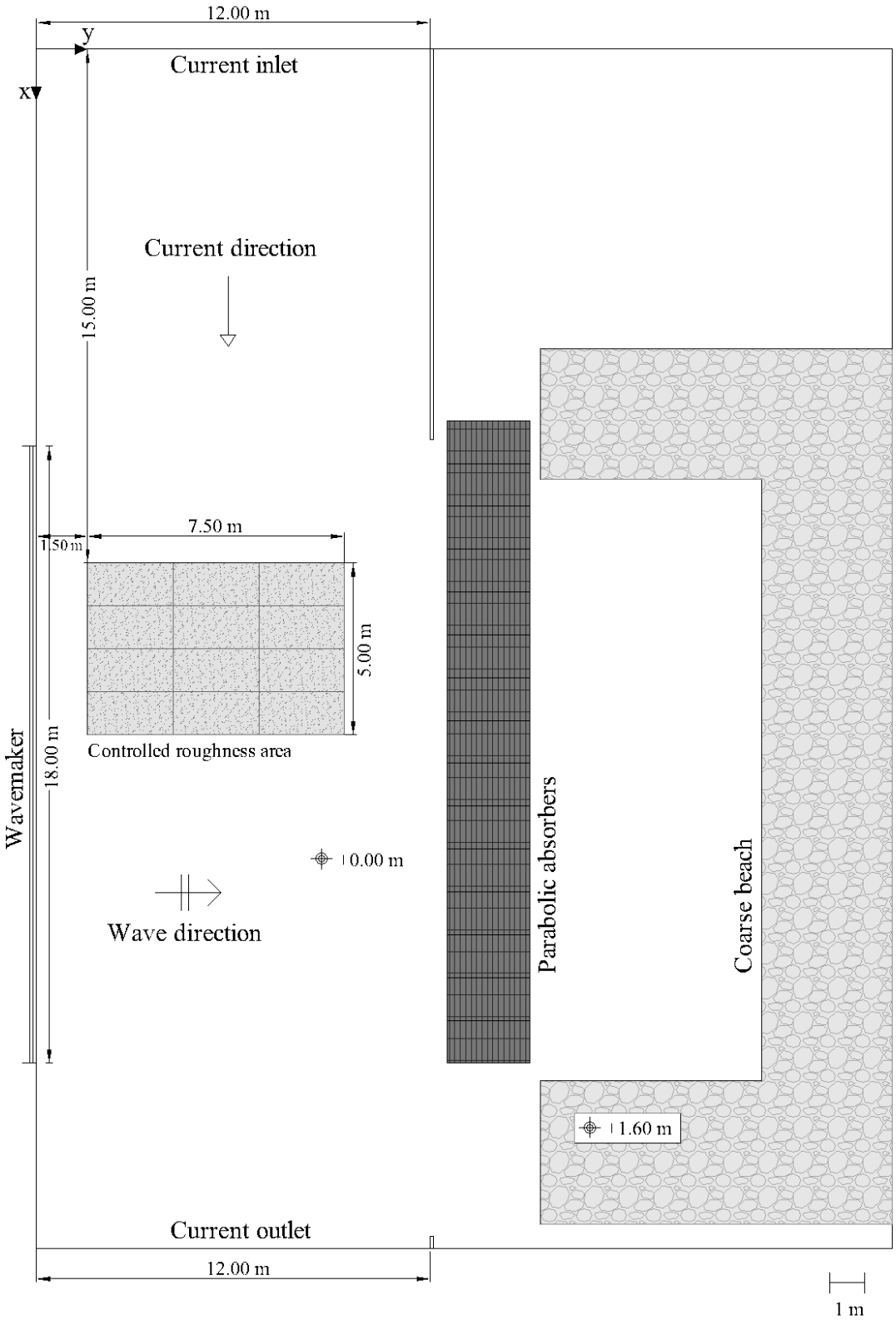

Figure 2: Top-view of the Shallow Water Basin.

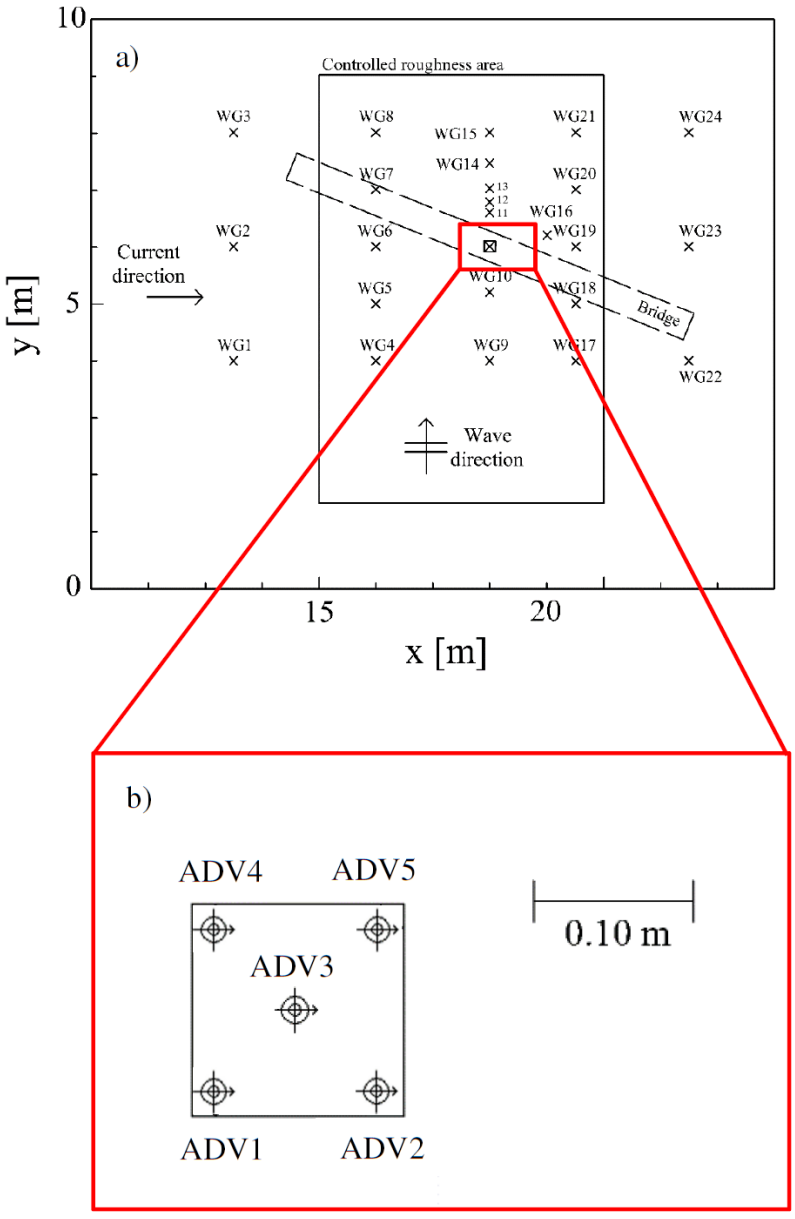

Figure 3: (a) Positioning of the wave gauges (crosses) and Acoustic Doppler Velocimeters (square) in the WINGS Shallow Water Basin; (b) close-up view of the ADV positioning.

Table 2: ADVs position in the Shallow Water Basin.

ADV	x [m]	y [m]
ADV1	17.88	5.88
ADV2	18.12	5.88
ADV3	18.00	6.00
ADV4	17.88	6.12
ADV5	18.12	6.12

Table 3: Experimental plan of the WINGS campaign.

Run	Type	h [m]	U [m/s]	H [m]	T [s]
Sand bed (SB)					
1	CO	0.40	0.21	-	-
2	WO	0.40	-	0.18	2.0
3	WO	0.40	-	0.12	2.0
4	WO	0.40	-	0.08	2.0
5	WO	0.40	-	0.08	1.0
6	WC	0.40	0.21	0.18	2.0
7	WC	0.40	0.21	0.12	2.0
8	WC	0.40	0.21	0.08	2.0
9	WC	0.40	0.21	0.08	1.0
Gravel bed (GB)					
28	WC	0.40	0.21	0.05	1.0
29	WO	0.40	-	0.08	2.0
30	WO	0.40	-	0.08	1.0
31	WO	0.40	-	0.05	1.0
32	CO	0.40	0.21	-	-
33	WC	0.40	0.21	0.08	2.0
34	WC	0.40	0.21	0.12	2.0
35	WC	0.40	0.21	0.08	1.0
36	WO	0.40	-	0.12	2.0

is the Vectrino, manufactured by Nortek (Nortek, 2009). The ADVs are held together onto a square chassis attached to a micrometer with a 0.0001 precision m, which allows them to be slided vertically. The micrometer is then fixed to a bridge above the acquisition area. The ADVs positioning is shown in Figure 3b. The ADVs are able to measure velocities within a cylindrical sampling volume of 0.001 m in height, with a resolution of 0.001 m/s, the accuracy is ±0.5% of the measured value. Sampling frequency is set to 200 Hz.

The data acquisition is remotely controlled by two terminals, one connected to the wave gauges data logger, collecting the water surface elevation, and one connected via USB to the ADVs, collecting flow velocity data. The wave gauges, the ADVs and the wavemaker are activated all together by means of the same signal from one of the two terminals, so that the measurements are synced with the start of the wavemaker movement. The ADVs position in the tank is shown in Figure 3b, their coordinates is shown in Table 2.

The performed experiments are listed in Table 3. The experimental plan included current only (CO), wave only (WO) and waves plus current (WC) conditions. A total of 18 runs have been carried out, Runs 9 over sand bed (SB) and 9 gravel bed (GB). A steady current has been generated with a mean current velocity of $U = 0.21$ m/s. A range of regular wave conditions have been carried out, with wave height H = $0.05 \div 0.18$ m and wave period T = $1 \div 2$ s.

Each Run consists of 16 tests, with each test having velocity measurements carried out at a different z, in order to recover 16 positions for each run with a specific wave-current configuration. During the same Run, wave and current conditions are unchanged. The measurement distance from the bed z for each Test is shown in Table 4. In order to achieve a steady current, the current recirculation system is activated 1 hour before starting the experiments. Sampling duration for CO Tests is equal to 2 minutes. Sampling duration of WO and WC Tests is 2 minutes for Tests with wave period $T = 1.0$ s and 4 minutes for Tests with $T = 2.0$ s, in order to collect 120 wave cycles. Wavemaker is turned on 2 minutes before the start of the sampling process in order to achieve a stable wave field.

Table 4: ADV measurement distance from the bed z for each Test.

Test	z [m]	Test	z [m]
1	0.001	9	0.025
2	0.002	10	0.035
3	0.003	11	0.050
4	0.005	12	0.075
5	0.008	13	0.120
6	0.011	14	0.150
7	0.015	15	0.200
8	0.020	16	0.250

Table 5: Dimensional and nondimensional parameters for the WINGS campaign Runs over sand bed: target current velocity U, wave height H, wave period T, current Reynolds number Re_c, wave Reynolds number Re_w, freestream current velocity U_c, orbital velocity U_w, wave-current regime parameter U_w/U_c.

Run	Bed	Type	U [m/s]	H [m]	T [s]	U_c [m/s]	U_w [m/s]	U_w/U_c	Re_c	Re_w
1	SB	CO	0.210	-	-	0.226	-	-	90225	-
2	SB	WO	-	0.18	2	-	0.412	-	-	54031
3	SB	WO	-	0.12	2	-	0.325	-	-	33621
4	SB	WO	-	0.08	2	-	0.218	-	-	15127
5	SB	WO	-	0.08	1	-	0.124	-	-	2447
6	SB	WC	0.210	0.18	2	0.237	0.387	1.63	94814	47645
7	SB	WC	0.210	0.12	2	0.242	0.319	1.32	96923	32350
8	SB	WC	0.210	0.08	2	0.239	0.203	0.85	95520	13066
9	SB	WC	0.210	0.08	1	0.223	0.107	0.48	89255	1819

METHODOLOGY

In the present work, the time-averaged velocities $\bar{u}$, $\bar{v}$ and $\bar{w}$, obtained by time-averaging the instantaneous velocities measured by all the ADVs, have been averaged in order to obtain time- and space-averaged $\langle\bar{u}\rangle$, $\langle\bar{v}\rangle$ and $\langle\bar{w}\rangle$ (referred in the text as double-averaging).

Dimensional and nondimensional parameters have been computed to characterize the flow field. Current freestream velocity has been computed by depth averaging the double-averaged current velocities above the expected current boundary layer upper limit ($z = 0.3h$). Wave orbital velocity has been computed by considering the phase-averaged velocity maximums at the first measurement point above the wave boundary layer thickness, computed according to Sleath (1987) as:

$$\delta_w = 3\sqrt{\frac{2\nu}{\omega}}. \tag{1}$$

where here ω is the wave angular frequency. Then, the orbital velocities measured by each ADV have been averaged in order to obtain double-averaged orbital velocity U_w.

Once U_c and U_w are obtained, current and wave Reynolds numbers have been computed by the following;

$$Re_c = \frac{U_c h}{\nu}; \qquad Re_w = \frac{U_w A}{\nu}; \tag{2}$$

where A is the wave orbital amplitude ($= U_w/\omega$). A nondimensional wave-current regime parameter U_w/U_c has been computed as an indicator of the relative importance of the waves compared to the current. Moreover, the wave-current parameter is used to distinguish two wave-current regimes: the current-dominated regime ($U_w/U_c < 1$) and the wave-dominated regime ($U_w/U_c > 1$). This is done in order to be consistent with literature (Lodahl et al., 1998) and facilitate the comparison. A range of dimensional quantities and parameters for each run is listed in Table 5 (runs over sand bed) and Table 6 (runs over gravel bed).

Current shear velocity (also referred as friction velocity) u^* and equivalent roughness k_s have been computed by best fit technique (Sumer, 2007). Such technique assumes that the shear velocity and equivalent roughness of a steady, fully developed boundary layer flow can be inferred by linear fitting the velocity profile in a certain region of the boundary layer, known as the logarithmic layer. Direct measurements of

Table 6: Dimensional and nondimensional parameters for the WINGS campaign runs over gravel bed: target current velocity U, wave height H, wave period T, current Reynolds number Re_c, wave Reynolds number Re_w, freestream current velocity U_c, orbital velocity U_w, wave-current regime parameter U_w/U_c.

Run	Bed	Type	U [m/s]	H [m]	T [s]	U_c [m/s]	U_w [m/s]	U_w/U_c	Re_c	Re_w
28	GB	WC	0.210	0.05	1	0.246	0.058	0.24	98286	534
29	GB	WO	-	0.08	2	-	0.199	-	-	12605
30	GB	WO	-	0.08	1	-	0.116	-	-	2142
31	GB	WO	-	0.05	1	-	0.061	-	-	592
32	GB	CO	0.210	-	-	0.245	-	-	97957	-
33	GB	WC	0.210	0.08	2	0.281	0.186	0.66	112209	11002
34	GB	WC	0.210	0.12	2	0.28	0.293	1.05	111937	27253
35	GB	WC	0.210	0.08	1	0.262	0.11	0.42	104742	1915
36	GB	WO	-	0.12	2	-	0.259	-	-	21290

Table 7: Quantities obtained through best fit procedure (Sumer, 2007): shear velocity u^*, equivalent roughness k_s and Reynolds shear number Re^*. Confidence intervals for u^* and k_s are also reported.

Run	u^* [m/s]	k_s [m]	Re^*
1	0.0109 ± 0.0009	0.0004 ± 0.0001	13
6	0.0128 ± 0.0021	0.0029 ± 0.0011	17
7	0.0115 ± 0.0015	0.0012 ± 0.0004	15
8	0.0124 ± 0.0013	0.0022 ± 0.0006	15
9	0.0120 ± 0.0014	0.0022 ± 0.0006	14
28	0.0265 ± 0.0054	0.1006 ± 0.0214	662
32	0.0242 ± 0.0070	0.0645 ± 0.0212	606
33	0.0284 ± 0.0024	0.0877 ± 0.0072	710
34	0.0286 ± 0.0013	0.0844 ± 0.0036	716
35	0.0273 ± 0.0031	0.0698 ± 0.0072	682

shear stresses has not been performed. Although advanced techniques and instruments exist (Musumeci et al., 2018; Stancanelli et al., 2020), most of them are not usable in large facilities such the one used in the current work, as they require close optical or electromagnetic monitoring which is not feasible in the present experimental setup. The best fit procedure is different depending if the flow is hydraulically smooth, i.e. when the viscous sublayer thickness is larger than the bed grain size, or is hydraulically rough, when the viscous sublayer is destroyed as the grains are fairly larger than the supposed thickness of the viscous. In hydraulically smooth flow, the velocity profile in the logarithmic region follows the law of the wall

$$\frac{u}{u^*} = \frac{1}{\kappa} log(\frac{zu^*}{\nu}) + 5.0 \tag{3}$$

where κ is the von Karman constant (= 0.4).

In hydraulically rough flow, the near-bed velocity distribution follows the following logarithmic law:

$$\frac{u}{u^*} = \frac{1}{\kappa} \ln \frac{z}{z_o} \tag{4}$$

where $z_0 = k_s/30$, where k_s is the equivalent roughness. Shear velocity is obtained from the slope of the linear fitting of u and $\log z$, whereas k_s is obtained through its intercept. However, an hypothesis on the position of the theoretical bottom must be done. The procedure again follows the one suggested by Sumer (2007).

From the shear velocity the Reynolds shear number has been computed, following the relation

$$Re^* = \frac{u^* d_{50}}{\nu}; \tag{5}$$

Table 7 shows u^*, k_s alongside their confidence interval values for all CO and WC runs. Confidence interval for u^* is in the average 12% with a maximum of 28% for Run 32.

All quantities are made dimensionless by dividing by the freestream velocity U_c.

RESULTS

In order to investigate the shear experienced by the current in proximity of the bed, the double-averaged profiles are analyzed specifically in the logarithmic layer region of the boundary layer.

Figure 4 shows a comparison between CO and WC dimensionless double-averaged velocity profiles, $\langle\bar{u}\rangle/U_c$ over sand bed (a) and over gravel bed (b) with $U = 0.210$ m/s in wall distance units z^+. The lines

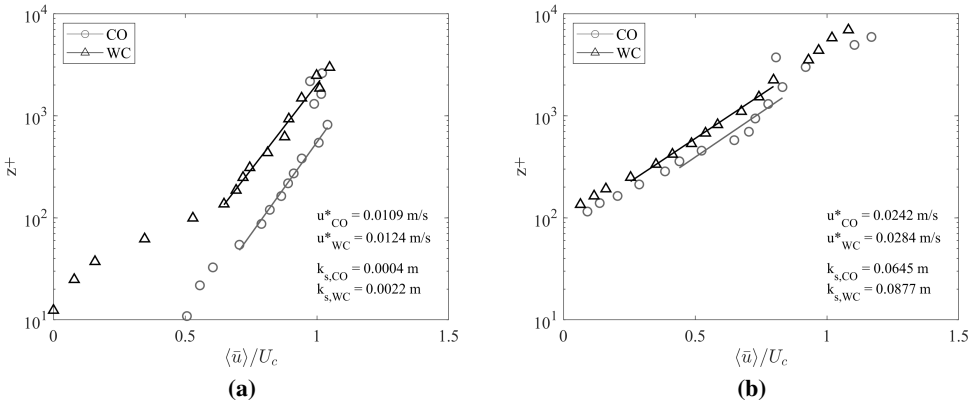

Figure 4: Logarithmic profiles in wall units with $U = 0.210$ m/s over sand bed: (a) Run 1 (CO, circles) and Run 8 (WC, triangles, $H = 0.08$ m, $T = 2.0$ s); (b) Run 32 (CO, circles) and Run 33 (WC, triangles, $H = 0.08$ m, $T = 2.0$ s).

denote the linear fitting used for the computation of u^* and k_s.

The two subfigures show that an increase of bottom friction is observed when waves are superposed to the steady current. This is probably determined by an increase of turbulent mixing induced by the superposition of the oscillatory flow. The shear velocity and equivalent roughness increase, as already predicted by previous studies (Grant and Madsen, 1979, 1986), although the in a lesser extent over a gravel bed.

Figure 5a shows Reynolds stress profiles of Run 1 (CO), Run 7 (WC, $H = 0.12$ m, $T = 2.0$ s) and Run 8 (WC, $H = 0.08$ m, $T = 2.0$ s), all runs are over sand bed with $U = 0.210$ m/s. The superposition of waves always induces an increment of bottom Reynolds stress. The Reynolds stress maximum is very close in values for both the WC cases, although the two peaks lies at a difference distance from the bed.

Figure 5b shows Reynolds stress profiles of Run 32 (CO), Run 33 (WC, $H = 0.08$ m, $T = 2.0$ s) and Run 34 (WC, $H = 0.12$ m, $T = 2.0$ s) over gravel bed with $U = 0.210$ m/s. The two WC Reynolds stress profile show a very similar behavior close to the surface. A greater shear stress maximum is associated with larger U_w/U_c case.

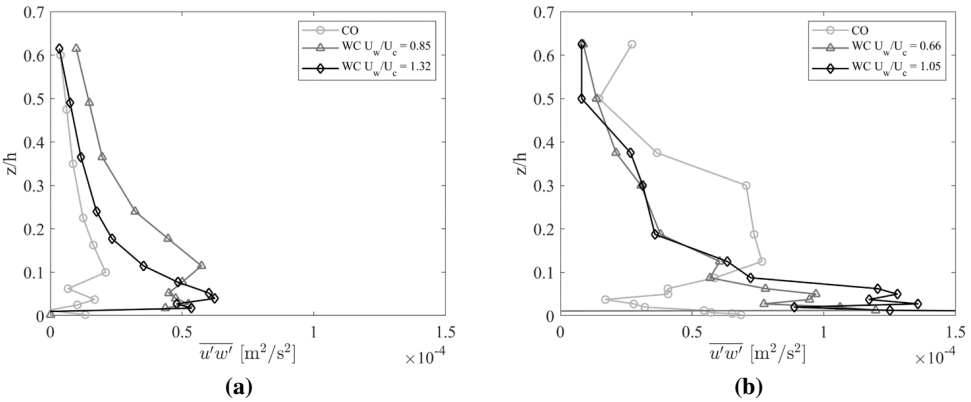

Figure 5: Reynolds stress profiles. (a) Run 1 (CO), Run 8 (WC, H = 0.08 m, T = 2.0 s) and Run 8 (WC, H = 0.08 m, T = 2.0 s), over sand bed with U = 0.210 m/s; (b) Run 32 (CO), Run 33 (WC, H = 0.08 m, T = 2.0 s) and Run 34 (WC, H = 0.12 m, T = 2.0 s) over gravel bed with U = 0.210 m/s.

CONCLUSIONS

In the present work, an investigation on the hydrodynamics of orthogonal wave-current combined flow has been carried out. Specifically, the work has been focused on the effects of waves on the current boundary layer, and on how the oscillatory flow affects the current velocity distribution. A laboratory campaign has been carried out, reproducing waves and currents propagating over sand and gravel flat beds. Flow velocity measurements have been carried out by means of Acoustic Doppler Velocimeters, both inside and outside of the boundary layer. Wave surface elevation time series have been measured by means of resistive wave gauges.

Mean flow has been investigated by computing double-averaged velocity profiles, by means of time- and space-averaging of the velocity time series for the WINGS dataset, and time-averaged profiles for the ACCLIVE dataset. Friction velocity and equivalent equivalent roughness have been inferred from the velocity profile by best fit method (Sumer, 2007). The hydrodynamics of the combined flow has been investigated by means of a comparison of the experiments of pure current with the ones in the presence of superposed waves. Instantaneous velocities have been Reynolds-averaged in order to obtain turbulent fluctuations time series, from which Reynolds stresses have been computed. The mean current velocity profiles of the WINGS dataset have been compared with a selection of analytical models in order to assess their validity for the case of wave-current orthogonal flow for the considered wave-current conditions. The data analysis of the laboratory experiments provided showed that The shear experienced by the flow in the current direction is always enhanced by the presence of the waves, as observed by the increment of friction velocity(up to 30%) and equivalent roughness (up to an order of magnitude). Such a result seems to be confirmed by the increase of Reynolds stresses in proximity of the bed, which are further enhanced by the larger roughness in the gravel bed case.

Future experimental studies should focus on: (i) extend the range of the experiments for the current U, (ii) recover direct measurements of bottom shear stresses rather than inferring via indirect methods, for instance by using innovative techniques, such as the one of Musumeci et al. (2018); (iii) further analysis on turbulence, including a phase-averaged Reynolds stress analysis, in order to better understand how the current bottom turbulent stress is altered during the different phases of the wave cycle.

ACKNOWLEDGEMENTS

This work has been partly funded by the project "NEWS - Nearshore hazard monitoring and Early Warning System" (code C1-3.2-60) in the framework of the programme INTERREG V-A Italia Malta 2014-2020, by University of Catania funded projects "Interazione onde correnti nella regione costiera (INOCS)", by the project eWAS "Early Warning System for Cultural Heritage" (PNR 2015-2020, cod. ARS01-00926), "Piano triennale della Ricerca 2016-18" and by POR SICILIA FSE (CCI: 2014IT05SFOP014).

References

K. H. Andersen and C. Faraci. The wave plus current flow over vortex ripples at an arbitrary angle. *Coastal engineering*, 47(4):431–441, 2003.

M. Arnskov, J. Fredsøe, and B. Sumer. Bed shear stress measurements over a smooth bed in three-dimensional wave-current motion. *Coastal Engineering*, 20(3-4):277–316, 1993.

W. Bakker. Sand concentration in an oscillatory flow. In *Coastal Engineering 1974*, pages 1129–1148. 1975.

W. T. Bakker and T. Van Doorn. Near-bottom velocities in waves with a current. In *Coastal Engineering 1978*, pages 1394–1413. 1978.

E. W. Bijker. The increase of bed shear in a current due to wave action. In *Coastal Engineering 1966*, pages 746–765. 1967.

J. B. Christoffersen and I. G. Jonsson. Bed friction and dissipation in a combined current and wave motion. *Ocean Engineering*, 12(5):387–423, 1985.

P. C. Fernando, J. Guo, and P. Lin. Wave–current interaction at an angle 1: experiment. *Journal of hydraulic research*, 49(4):424–436, 2011.

J. Fredsøe. Turbulent boundary layer in wave-current motion. *Journal of Hydraulic Engineering*, 110(8): 1103–1120, 1984.

W. D. Grant and O. S. Madsen. Combined wave and current interaction with a rough bottom. *Journal of Geophysical Research: Oceans*, 84(C4):1797–1808, 1979.

W. D. Grant and O. S. Madsen. The continental-shelf bottom boundary layer. *Annual review of fluid mechanics*, 18(1):265–305, 1986.

F. Havinga. Sediment concentrations and sediment transport in case of irregular non-breaking waves with a current. 1992.

P. Kemp and R. Simons. The interaction between waves and a turbulent current: waves propagating with the current. *Journal of Fluid Mechanics*, 116:227–250, 1982.

P. Kemp and R. Simons. The interaction of waves and a turbulent current-waves propagating against the current. *J Fluid Mech*, 130(MAY):73–89, 1983.

K. Y. Lim and O. S. Madsen. An experimental study on near-orthogonal wave–current interaction over smooth and uniform fixed roughness beds. *Coastal Engineering*, 116:258–274, 2016.

C. Lodahl, B. M. Sumer, and J. Fredsøe. Turbulent combined oscillatory flow and current in a pipe. *Journal of Fluid Mechanics*, 373:313–348, 1998.

M. Marino, C. Faraci, and R. E. Musumeci. An experimental setup for combined wave-current flow interacting at a right angle over a plane beach. *Italian Journal of Engineering Geology and Environment*, 1: 99–106, 2020a.

M. Marino, C. Faraci, and R. E. Musumeci. Shoaling waves interacting with an orthogonal current. *Journal of Marine Science and Engineering*, 8(4):281, 2020b.

P. P. Mathisen and O. S. Madsen. Waves and currents over a fixed rippled bed: 2. bottom and apparent roughness experienced by currents in the presence of waves. *Journal of Geophysical Research: Oceans*, 101(C7):16543–16550, 1996a.

P. P. Mathisen and O. S. Madsen. Waves and currents over a fixed rippled bed: 1. bottom roughness experienced by waves in the presence and absence of currents. *Journal of Geophysical Research: Oceans*, 101(C7):16533–16542, 1996b.

R. Musumeci, L. Cavallaro, E. Foti, P. Scandura, and P. Blondeaux. Waves plus currents crossing at a right angle: Experimental investigation. *Journal of Geophysical Research: Oceans*, 111(C7), 2006.

R. E. Musumeci, V. Marletta, A. Sanchez-Arcilla, and E. Foti. A ferrofluid-based sensor to measure bottom shear stresses under currents and waves. *Journal of Hydraulic Research*, 56(5):630–647, 2018.

A. Nortek. Vectrino velocimeter user guide. *Nortek AS, Vangkroken, Norway*, 621, 2009.

J. Sleath. Turbulent oscillatory flow over rough beds. *Journal of Fluid Mechanics*, 182:369–409, 1987.

J. Sleath. Velocities and bed friction in combined flows. In *Coastal Engineering 1990*, pages 450–463. 1991.

L. Stancanelli, R. E. Musumeci, M. Stagnitti, and E. Foti. Optical measurements of bottom shear stresses by means of ferrofluids. *Experiments in Fluids*, 61(2):52, 2020.

B. Sumer. Lecture notes on turbulence/technical university of denmark, 2007, 2007.

P. J. Visser. Wave basin experiments on bottom friction due to current and waves. In *Coastal Engineering 1986*, pages 807–821. 1987.

J. Yuan and O. S. Madsen. Experimental study of turbulent oscillatory boundary layers in an oscillating water tunnel. *Coastal engineering*, 89:63–84, 2014.